Exclusion of Six-Coordinate Intermediates in the Electrochemical Reduction of CO_2 Catalyzed by [Pd(triphosphine)(CH_3CN)](BF_4)$_2$ Complexes

Paul R. Bernatis, Alex Miedaner, R. Curtis Haltiwanger,† and Daniel L. DuBois*

National Renewable Energy Laboratory, Golden, Colorado 80401

Received May 18, 1994®

[Pd(triphosphine)(CH_3CN)](BF_4)$_2$ complexes have been prepared with mesityl or trimethoxybenzene substituents on the central phosphorus atom of the triphosphine ligand. An X-ray diffraction study of [Pd(MesetpE)(CH_3CN)](BF_4)$_2$ (where MesetpE is bis((diethylphosphino)ethyl)mesitylphosphine) has been completed. [Pd(MesetpE)(CH_3CN)](BF_4)$_2$ crystallizes in the space group $P\bar{1}$ with a = 10.370(2) Å, b = 11.009(2) Å, c = 14.483(2) Å, α = 103.203(13)°, β = 92.748(16)°, γ = 92.556(15)°, V = 1605.2(5) Å^3, and Z = 2. The structure was refined to R = 0.0659 and R_w = 0.0771 for 4467 independent reflections with $F > 4\sigma(F)$. The cation has a square-planar structure with one methyl group of the central mesityl substituent blocking one potential coordination site. Kinetic studies of this complex in dimethylformamide indicate that the rate-determining step is the reaction of the [Pd(MesetpE)(DMF)]$^+$ cation with CO_2. Comparison of the rate constants for this and other mesityl-substituted complexes with those of other [Pd(triphosphine)(CH_3CN)](BF_4)$_2$ complexes suggests that all proceed through a five-coordinate transition state.

Introduction

There is currently considerable interest in the chemistry of carbon dioxide due to its role in the greenhouse effect and the possibility of using CO_2 as a chemical feedstock. Various aspects of this chemistry have been summarized in a number of recent reviews.[1] Of the structurally characterized CO_2 complexes,[2] a significant portion contain phosphine ligands.[3] However, only a few transition-metal phosphine complexes catalyze the electrochemical reduction of CO_2.[4] Recent research in our laboratories has focused on developing catalysts of this type. In this effort, a number of transition-metal complexes containing polyphosphine ligands and weakly coordinating solvent molecules were prepared and evaluated for their ability to catalyze electrochemical CO_2 reduction.[5,6] By using bidentate, tridentate, and tetradentate polyphosphine ligands, the number of solvent molecules bound to the metal could be systematically varied. This approach permitted optimization of the number of potentially vacant coordination sites. A second objective was to take advantage of the chelate effect of polyphosphine ligands to minimize metal–phosphorus bond-cleavage reactions. Such reactions would be expected to compete with CO_2 reduction and lead to catalyst deactivation.

During the course of this research, it was found that [Pd(triphosphine)(CH_3CN)](BF_4)$_2$ complexes catalyze the reduction of CO_2 to CO in acidic dimethylformamide and acetonitrile solutions.[7] These [Pd(triphosphine)(CH_3CN)](BF_4)$_2$ catalysts exhibit a number of interesting properties: (1) They are relatively fast compared to other homogeneous catalysts for CO_2 reduction. (2) They can be quite selective for CO production even in moderately acidic solutions. (3) They operate at relatively positive potentials. On the negative side, these catalysts, like many homogeneous catalysts, are relatively fragile and exhibit low turnover numbers—typically between 10 and 100. To improve the rates, selectivity, and stability of these catalysts, the relationship between structure and reactivity is being investigated. In this study, advantage is taken of the ability to control coordination numbers of metal complexes with polydentate ligands to probe the coordination number of the transition states and intermediates in the catalytic cycle.

On the basis of our mechanistic studies, a five-coordinate palladium(I) complex, **1**, has been proposed as the transition state for the rate-determining step in the catalytic cycle.[7] A similar structure was suggested

† Department of Chemistry and Biochemistry, University of Colorado, Boulder, CO 80309.

® Abstract published in *Advance ACS Abstracts,* November 1, 1994.

(1) For general reviews of CO_2 chemistry see: Behr, A. *Carbon Dioxide Activation by Metal Complexes*, VCH: New York, 1988. Braunstein, P.; Matt, D.; Nobel, D. *Chem. Rev.* **1988**, *88*, 747–764. For reviews of electrochemical reduction of CO_2 see: *Electrochemical and Electrocatalytic Reactions of Carbon Dioxide*; Sullivan, B. P.; Krist, K.; Guard, H. E.; Eds.; Elsevier: New York, 1993. Collin, J.-P.; Sauvage, J.-P. *Coord. Chem. Rev.* **1989**, *93*, 245–268.

(2) Creutz, C. *Electrochemical and Electrocatalytic Reactions of Carbon Dioxide*; Sullivan, B. P.; Krist, K.; Guard, H. E.; Eds.; Elsevier: New York, 1993, p 19.

(3) Aresta, M.; Nobile, C. F.; Albano, V. G.; Forni, E.; Manassero, M. *J. Chem. Soc., Chem. Commun.* **1975**, *98*, 1615, 7405. Alvarez, R.; Camona, E.; Marin, J. M.; Poveda, M. L.; Cutierrez-Puebla, E.; Monge, A. *J. Am. Chem. Soc.* **1986**, *108*, 2286. Bristow, G. S.; Hitchcock, P.; Lappert, M. F. *J. Chem. Soc., Chem. Commun.* **1981**, 1145. Herskovitz, T.; Guggenberger, L. J. *J. Am. Chem. Soc.* **1976**, *98*, 1615. Calabrese, J. C.; Herskovitz, T.; Kinney, J. B. *J. Am. Chem. Soc.* **1973**, *105*, 5914.

(4) Slater, S.; Wagenknecht, J. H. *J. Am. Chem. Soc.* **1984**, *106*, 5367. Miloslavjevic, E. B.; Solujic, L.; Krassowski, D. W.; Nelson, J. H. *J. Organomet. Chem.* **1988**, *352*, 177. Ratliff, K. S.; Lentz, R. E.; Kubiak, C. P. *Organometallics* **1992**, *11*, 1986.

(5) DuBois, D. L.; Miedaner, A. *Catalytic Activation of Carbon Dioxide*; Ayers, W. M., Ed.; ACS Symposium Series 363; American Chemical Society: Washington, DC, 1988; p 42. DuBois, D. L.; Miedaner, A. *Inorg. Chem.* **1986**, *25*, 4642. Miedaner, A.; DuBois, D. L. *Ibid.* **1988**, *27*, 2479.

(6) DuBois, D. L.; Miedaner, A. *J. Am. Chem. Soc.* **1987**, *109*, 113.

(7) DuBois, D. L.; Miedaner, A.; Haltiwanger, R. C. *J. Am. Chem. Soc.* **1991**, *113*, 8753.

0276-7333/94/2313-4835$04.50/0

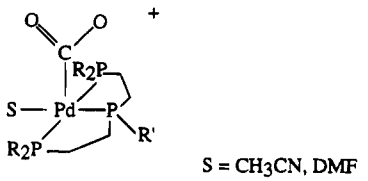

S = CH_3CN, DMF

1

by Sauvage and co-workers for $[Ni(cyclam)(CO_2)]^+$.[8] In the latter system, adsorption of $[Ni(cyclam)]^+$ on mercury was proposed to play an important role in the catalytic process. Subsequent electrochemical studies have confirmed the importance of adsorption[9] and led Anson and co-workers to suggest an octahedral coordination environment for the adsorbed Ni(I)-CO_2 complex.[10] A similar conclusion was reached by Sakaki on the basis of *ab initio* molecular orbital calculations on Ni^I–CO_2 complexes.[11] These studies raised the possibility that six-coordinate intermediates may be involved in the catalytic reactions of the palladium triphosphine complexes. Even if such species are not normally involved in the catalytic cycle, increasing the probability for octahedral coordination might enhance the catalytic rate. This paper describes the synthesis and electrochemical studies of complexes designed to test these ideas by preventing and promoting coordination of a sixth ligand in intermediates such as **1**.

Experimental Section

Physical Measurements and General Procedures. ^1H and ^{31}P NMR spectra were recorded on a Varian Unity 300 MHz spectrometer at 299.75 and 121.42 MHz, respectively. ^1H chemical shifts are reported relative to tetramethylsilane using residual solvent protons as a secondary reference. ^{31}P chemical shifts are reported relative to external phosphoric acid. Infrared spectra were recorded on a Nicolet 510P spectrometer. Elemental analyses were performed by Schwarzkopf Laboratories, Woodside, NY. All syntheses were carried out using standard Schlenk and drybox techniques. Electrochemical experiments were carried out under either N_2 or CO_2 atmospheres as specified below.

$[Pd(MesetpE)(CH_3CN)](BF_4)_2$ crystallized at room temperature over a 3-week period from an acetonitrile/diethyl ether solution maintained under a nitrogen atmosphere. The crystals were mounted with epoxy on glass fibers. Repeated attempts to collect data at −100 °C were unsuccessful because the crystals fractured as they cooled. X-ray crystallographic measurements were carried out on a Siemens P3/F autodiffractometer. Mo Kα radiation (monochromatized by diffraction off a highly oriented graphite crystal) was used in this study. Programs in the Siemens X-ray package were used for data collection and for structure solution and refinement. Details of the experimental conditions are given in the supplementary material. Table 1 summarizes the crystal data for $[Pd(MesetpE)(CH_3CN)](BF_4)_2$.

Cyclic voltammetry experiments were carried out on a Cypress Systems computer-aided electrolysis system equipped with a CYSY 1r potentiostat. The working electrode was a glassy-carbon disk (1-mm diameter, Cypress Systems EE005). The counter electrode was a glassy-carbon rod (1-mm diameter), and a silver wire coated with AgCl was used as a pseudo reference electrode to fix the potential. Ferrocene was used as an internal standard, and all potentials are referenced to the ferrocene/ferrocenium couple.[12] Controlled-potential electrolysis experiments were performed with a Princeton Applied Research Model 173 potentiostat equipped with a Model 179 digital coulometer and a Model 175 universal programmer. Working electrodes were constructed from vitreous carbon cylinders (60 pores/in., Electrosynthesis Corp., 14-mm diameter). Electrical contact between the copper lead and the reticulated vitreous carbon was made with silver epoxy (Johnson Matthey). These electrodes were inserted into the solutions to be electrolyzed to a depth of 10 mm. The counter electrode was a tungsten wire. A silver wire immersed in an acetonitrile solution containing 1.5×10^{-3} M permethylferrocene and 1.5×10^{-3} M permethylferrocenium tetrafluoroborate was used to establish a reference potential.[13] The reference and counter electrodes were separated from the working electrode compartment by Vycor frits (7-mm diameter, 1-mm thick). All electrochemical experiments were carried out in 0.1 M Et_4NBF_4 dimethylformamide solutions unless noted otherwise.

Table 1. Crystal Data, Data Collection Conditions, and Solution Refinement Details for $[Pd(MesetpE)(CH_3CN)](BF_4)_2$ (7a)

empirical formula	$C_{23}H_{42}B_2NF_8P_3Pd$
color, habit	clear, colorless parallelepiped
crystal dimens	0.40 × 0.45 × 0.50 mm
space group	$P\bar{1}$
cryst syst	triclinic
unit cell dimensions	
a	10.370(2) Å
b	11.009(2) Å
c	14.483(2) Å
α	103.203(13)°
β	92.748(16)°
γ	92.556(15)°
V	1605.2(5) Å^3
Z	2
d_{calc}	1.460 g/cm^3
fw	705.5
abs coeff	0.776 mm^{-1}
radiation	Mo Kα (λ = 0.710 73 Å)
temp	22−24 °C
final residuals (obsd data)	R = 5.27%, R_w = 7.32%
residuals (all data)	R = 6.59%, R_w = 7.71%

Controlled-Potential Electrolysis of $[Pd(triphosphine)(CH_3CN)](BF_4)_2$ Complexes under Nitrogen. The controlled-potential electrolysis of $[Pd(Mesetp)(CH_3CN)](BF_4)_2$ (where Mesetp is bis((diphenylphosphino)ethyl)mesitylphosphine) is typical of the procedure used for the electrolysis of other $[Pd(triphosphine)(CH_3CN)](BF_4)_2$ complexes. $[Pd(Mesetp)(CH_3CN)](BF_4)_2$ (0.010 g, 0.011 mmol) was dissolved in 10 mL of a 0.1 M Et_4NBF_4/DMF solution. Nitrogen was bubbled through the solution for 1 h, and then the electrochemical cell was sealed. The reaction was stirred at room temperature while the potential of the working electrode was maintained at −1.18 V (100 mV negative of $E_{1/2}$). As the electrolysis proceeded, the solution became dark brown. The reaction was stopped after the current fell to ~5% of its original value. The ratio of the faradays of charge passed to the moles of complex is reported in Table 5 as n. The volume of the reaction mixture was reduced in a vacuum until 1 mL of solvent remained, and a ^{31}P NMR spectrum of the product mixture was recorded. For the compounds where R = Mes, R′ = Et and R = Mes, R′ = Ph, complex mixtures of products were observed. For the compound where R = Mes and R′ = Cy, the ^{31}P NMR spectrum contained two poorly resolved resonances at 94.9 and 62.0 ppm. The ^{31}P NMR spectrum of the product mixture from the reduction of $[Pd(TMBetpE)(CH_3CN)](BF_4)_2$ (where TMBetpE is bis((diethylphosphino)ethyl)-

(8) Beley, M.; Collin, J.-P.; Ruppert, R.; Sauvage, J.-P. *J. Am. Chem. Soc.* **1986**, *108*, 7461.
(9) Fujihira, M.; Hirata, Y.; Suga, K. *J. Electroanal. Chem.* **1990**, *292*, 199.
(10) Balazs, G. B.; Anson, F. C. *J. Electroanal. Chem.* **1992**, *322*, 325.
(11) Sakaki, S. *J. Am. Chem. Soc.* **1992**, *114*, 2055.
(12) Gagne, R. R.; Koval, C. A.; Lisensky, G. C. *Inorg. Chem.* **1980**, *19*, 2855. Gritzner, G.; Kuta, J. *Pure Appl. Chem.* **1984**, *56*, 461. Hupp, J. T. *Inorg. Chem.* **1990**, *29*, 5010.
(13) Bashkin, J. K.; Kinlen, P. *Inorg. Chem.* **1990**, *29*, 4507.

(2,4,6-trimethoxyphenyl)phosphine) contained resonances for the unreduced starting materials in addition to resonances for other compounds that were not further characterized.

Determination of Rate Constants. Catalytic rates were determined using eq 4 or 5 in the text. A typical procedure for determining the rate constant is given for $[Pd(MesetpE)(CH_3CN)](BF_4)_2$. The value of the peak current, i_p, was determined by preparing five DMF solutions of $[Pd(MesetpE)(CH_3CN)](BF_4)_2$ with concentrations between 6.8×10^{-3} and 1.7×10^{-3} M. Each solution was saturated with CO_2 (0.18 M) at ambient temperature (21 ± 1 °C) and atmospheric pressure (620 ± 20 mmHg),[14] and the potential of the working electrode was scanned at 20 mV/s. Peak currents were plotted vs catalyst concentration, and the slope was calculated to be 0.58 μA/mM. The catalytic current, i_c, was measured in the same manner for DMF solutions containing HBF_4 (0.1 M), $[Pd(MesetpE)(CH_3CN)](BF_4)_2$ (8×10^{-4} to 2×10^{-4} M), and CO_2 (620 mmHg). A slope of 7.8 μA/mM was determined from a plot of peak current vs concentration of $[Pd(MesetpE)(CH_3CN)](BF_4)_2$. Rate constants are given in Table 5. $E_{1/2}$ values for the catalysts were measured using the potential at half-height of the catalytic waves[15] and are reported in Table 5.

Determination of Current Efficiencies in Dimethylformamide. In a typical experiment, 10 mL of a dimethylformamide solution containing 1×10^{-3} M $[Pd(triphosphine)(CH_3CN)](BF_4)_2$, 0.1 M HBF_4, and 0.1 M Et_4NBF_4 was saturated with CO_2 at ambient temperature and atmospheric pressure. The electrolysis cell was sealed, and the solution was stirred while maintaining the potential 100 mV negative of the $E_{1/2}$ value of the catalyst. Gaseous samples (100 μL) were taken at intervals of 10 C, and H_2 and CO yields were determined by gas chromatography. Catalytic efficiencies and the number of catalyst turnovers are given in Table 5. No attempts were made to optimize catalyst lifetimes, and the values recorded were calculated after the current had dropped to 10–20% of its original value. The same conditions were also used for experiments carried out in DMF in which 0.1 M H_3PO_4 was substituted for HBF_4.

Effect of Formic Acid and Dimethylamine on Current Efficiencies. Formic acid (3.7 μL, 0.098 mmol) was added to a DMF solution (10 mL) containing 0.1 M HBF_4, 0.1 M Et_4NBF_4, and 1.0×10^{-3} M $[Pd(MetpC)(CH_3CN)][BPh_4]_2$ (where MetpC is bis((dicyclohexylphosphino)ethyl)methylphosphine). CO_2 was bubbled through the mixture for 30 min, and the electrochemical cell was sealed. The reaction mixture was electrolyzed at −1.6 V. The current efficiencies for CO and H_2 were 74% and 30%, respectively. Under the same conditions, with the exception of replacing the formic acid solution with a 1×10^{-2} M $(CH_3)_2NH$ solution, the current efficiencies for CO and H_2 were 94% and 11%, respectively.

Determination of Current Efficiencies in Propylene Carbonate. A solution of $[Pd(etpC)(CH_3CN)][BPh_4]_2$ (where etpC is bis((dicyclohexylphosphino)ethyl)phenylphosphine) in 10 mL of propylene carbonate was prepared as described for catalytic experiments in DMF. The electrochemical cell was equipped as in other controlled-potential experiments except electrical contact was made to the working electrode by a graphite rod (1-cm diameter) connected to the reticulated vitreous carbon by silver epoxy. The reaction mixture was purged with CO_2 and the solution electrolyzed as described above. The current efficiencies for CH_4, CO, and H_2 were 11%, 14%, and 80%, respectively. In the presence of a 13/1 $^{12}CO_2/^{13}CO_2$ mixture, the molar ratio of $^{12}CH_4/^{13}CH_4$ formed was 13/1 as determined by GC/MS. Control experiments (1–d) were carried out as described in the preceding paragraph with the following changes. (a) The catalyst $[Pd(etpC)(CH_3CN)][BPh_4]_2$ was absent. (b) A nonmetallic epoxy was substituted for silver epoxy. (c) The working electrode was replaced with an electrode constructed from silver wire (1-mm diameter) wound into a coil (8-mm diameter, 3 mm long). (d) N_2 or CO was substituted for CO_2. Methane was not detected in any of these control experiments.

Materials. Vinylmagnesium bromide, PCl_3, trimethoxybenzene, and mesitylmagnesium bromide were purchased from Aldrich. Matheson Bone Dry carbon dioxide was used in all electrolysis experiments. Diphenylphosphine, diethylphosphine, dicyclohexylphosphine, and divinylphenylphosphine were purchased from Strem Chemicals and were used as received. Tetrahydrofuran and diethyl ether were distilled from sodium benzophenone ketyl, and acetonitrile was distilled from calcium hydride. Dimethylformamide and propylene carbonate were purchased from Burdick and Jackson and stored under nitrogen. Et_4NBF_4 was recrystallized from ethanol and dried under vacuum at 100 °C for 1 day. The complexes $[RP(CH_2CH_2PR'_2)_2Pd(CH_3CN)](BF_4)_2$, where R is other than mesityl or 2,4,6-trimethoxyphenyl, have been synthesized previously.[7] $[Pd(CH_3CN)_4](BF_4)_2$,[16] dichloromesitylphosphine ($MesPCl_2$),[17] and divinyl(diethylamino)phosphine[18] were prepared by literature methods.

Syntheses. Divinylmesitylphosphine (2). Dichloromesitylphosphine (8.18 g, 0.037 mol) was dissolved in tetrahydrofuran (50 mL), and the solution was cooled to −78 °C. Vinylmagnesium bromide (80 mL of a 1 M tetrahydrofuran solution, 0.08 mol) was added slowly over 1.5 h, resulting in a white precipitate. The solution was warmed slowly to room temperature and stirred for 18 h. The solvent was removed by distillation at atmospheric pressure. The residue was extracted with pentane (3 × 35 mL), and the combined extracts were distilled. The fraction distilling between 63 and 65 °C at 4.6×10^{-5} atm was collected (2.8 g, 38%). ^1H NMR (toluene-d_8): $(CH_3)_3C_6H_2$, 6.85–6.84 ppm (m); $CH{=}CH_2$, 6.63–6.46, 5.65–5.41 ppm (m's); *o*-CH_3 2.60 ppm (s), *p*-CH_3, 2.20 ppm (s). ^{31}P NMR (toluene-d_8): −24.54 ppm (s).

$RP(CH_2CH_2PR'_2)_2$ (R = Mes, R' = Et (3a), Ph (3b), Cy (3c); R = Et_2N, R' = Et (4)). In a typical procedure divinylmesitylphosphine (1.0 g, 4.9 mmol), R_2PH (1.0–2.0 g, 12 mmol), and AIBN (0.1 g) were combined in a Schlenk flask and irradiated in a Rayonet reactor using lamps with 254 and 350 nm wavelengths. The reaction was periodically monitored by ^{31}P and ^1H NMR. For R = Mes and R' = Et, Ph, and Cy, the reactions went to completion after 2.5, 0.75, and 6 days, respectively. For R = Et_2N and R' = Et, the reaction time was 3 days. The product mixtures were heated to between 100 and 200 °C under dynamic vacuum to remove excess phosphine. The products were used without further purification. Crude yields varied from 57 to 83%. ^1H NMR and ^{31}P NMR data are recorded in Table 2.

$CH_3OP(PCH_2CH_2PEt_2)_2$ (5). $Et_2NP(CH_2CH_2PEt_2)_2$ (7.0 g, 21 mmol) was dissolved in 30 mL of dry methanol and stirred at 60 °C for 2 h. The solvent was removed in a vacuum at room temperature to produce a clear oil (5.75 g, 93%). ^1H NMR and ^{31}P NMR data are recorded in Table 2.

$[MesP(CH_2CH_2PR_2)_2Pd(CH_3CN)](BF_4)_2$ (R = Et (7a), Ph (7b), Cy (7c)). The procedure for the complex where R = Ph is typical of those used to prepare all of the palladium complexes. A solution of $MesP(CH_2CH_2PPh_2)_2$ (1.8 g, 2.8 mmol) in tetrahydrofuran (30 mL) was added to a solution of $[Pd(CH_3CN)_4](BF_4)_2$ (1.27 g, 2.9 mmol) in acetonitrile (30 mL). The resulting yellow solution was stirred for 1 h, and the solvent was removed at reduced pressure to give a yellow oily solid. The yellow, phenyl-substituted complex and the orange, ethyl-substituted complex were recrystallized from mixtures of acetonitrile and diethyl ether in 50–70% yields. Numerous attempts to recrystallize the orange cyclohexyl analogue were

(14) *Solubilities of Inorganic and Organic Compounds*; Stephen, H., Stephen, T., Eds.; Pergamon: New York, 1958; Vol. 1, p 1063.
(15) Savéant, J. M.; Vianello, E. *Electrochim. Acta* **1963**, *8*, 905.
(16) Sen, A.; Ta-Wang, L. *J. Am. Chem. Soc.* **1981**, *103*, 4627. Hathaway, B. J.; Holah, D. G.; Underhill, A. E. *J. Chem. Soc.* **1962**, 2444.
(17) Oshikawa, T.; Yamashita, M. *Chem. Ind. (London)* **1985**, 126.
(18) King, R. B.; Master, W. F. *J. Am. Chem. Soc.* **1977**, *99*, 4001.

Table 2. NMR Data for Ligands and Complexes

	$^{31}P^a$			$^1H^b$				
				R				
compd	δ_c(calcd)[c] triplet	δ_t(calcd)[c] doublet	J (Hz)	CH_3[e] or OCH_3	$C_6H_2(CH_3)_3$[f] or $C_6H_2(OCH_3)_3$	CH_2CH_2	R′	CH_3CN[d]
3a	−21.4 (−21)	−18.4 (20)	26	2.08 (*p*), 2.61 (*o*)	6.73−6.74	1.33−2.21	0.9−1.0 (m, CH_2CH_3), 1.16−1.26 (m, CH_2CH_3)	
3b	−21.5 (−21)	−11.6 (−12)	35	2.04 (*p*), 2.39 (*o*)	6.64−6.65	2.2−1.7	7.4−6.9 (m, C_6H_5)	
3c	−21.4 (−21)	0.8 (0)	30	2.06 (*p*), 2.61 (*o*)	6.72−6.73	2.1−2.9	1.05−1.85 (m, C_6H_{11})	
4	61.6	−17.6 (−20)	22	0.98 (t), 2.86 (dq)	$N(CH_2CH_3)_2$ (J = 7 Hz), $N(CH_2CH_3)_2$ (J_{PH} = 9 Hz)	1.3−1.7	0.95−1.1 (m, CH_2CH_3), 1.2−1.3 (m, CH_2CH_3)	
5	139.8	−18.2 (−20)	20	3.38 (d)	OCH_3 (J = 13 Hz)	1.4−1.8	0.9−1.1 (m, CH_2CH_3), 1.15−1.3 (m, CH_2CH_3)	
6	−29.4	−17.8 (−20)	22					
7a	96.1	60.0	4	2.31, 2.57, 2.84	7.12−7.16	1.7−3.2	1.1−1.3 (m, CH_2CH_3), 2.2−2.3 (m, CH_2CH_3)	1.95 (2.57)
7b	99.5	52.0	3	2.24 (*p*), 2.57 (*o*)	6.88, 7.14	2.6−3.4	7.5−7.7 (C_6H_5)	1.95 (2.31)
7c	98.7	70.7	0	2.30, 2.55, 2.93	7.12−7.15	2.1−3.2	1.2−1.9 (C_6H_{11})	1.95 (2.65)
7d	92.1	61.7	5	3.88 (*p*), 3.90 (*o*)	6.32, 6.31	1.6−3.2	1.07−1.30 (m, CH_2CH_3), 2.10−2.20 (m, CH_2CH_3)	1.95 (2.35)

[a] All ^{31}P NMR chemical shifts are referenced to external H_3PO_4. [b] All proton NMR chemical shifts are given in ppm relative to TMS using residual proton solvent resonances as secondary references. Spectra for all complexes were recorded in acetonitrile-d_3. Spectra for the ligands were recorded in toluene-d_8. [c] Chemical shifts are calculated using eq 2 on p 89 of ref 19 and substituent parameters from refs 19 and 7. [d] Values in parentheses are for coordinated acetonitrile in nitromethane-d_3 solutions. [e] All methyl and methoxy resonances are singlets. [f] These resonances are all multiplets.

Table 3. Elemental Analysis and Infrared Data for $[RP(CH_2CH_2PR'_2)_2Pd(CH_3CN)](BF_4)_2$ Complexes

		calcd (%)				found (%)				
R, R′	formula	C	H	N	P	C	H	N	P	IR (cm^{-1})[a] ν_{CN}
Mes, Et	$C_{23}H_{42}P_3NPdB_2F_8$	39.15	6.00	1.99	13.17	39.70	6.01	2.35	14.04	2320, 2293
Mes, Cy	$C_{39}H_{66}P_3NPdB_2F_8$	50.81	7.22	1.51	10.08	48.49	6.73	2.32	9.11	2321, 2292
Mes, Ph	$C_{39}H_{42}P_3NPdB_2F_8$	52.18	4.72	1.56	10.35	52.51	4.96	1.89	10.01	2318, 2290
TMB, Et	$C_{23}H_{42}P_3NPdO_3B_2F_8$	36.66	5.62	1.86	12.33	36.51	5.55	1.91	11.96	2332, 2305[b]

[a] Spectra recorded in dichloromethane. [b] Nujol mull.

unsuccessful. Characterization data for these complexes are given in Tables 2 and 3.

$[TMBP(CH_2CH_2PEt_2)_2Pd(CH_3CN)](BF_4)_2$ (7d). A solution of lithium trimethoxybenzene (4.0 mmol) in THF (30 mL) was prepared by reacting butyllithium in THF (4 mL of a 1 M solution) with trimethoxybenzene (0.67 g, 4.0 mmol) in THF (25 mL). This solution was added by cannula to a solution of $CH_3OP(CH_2CH_2PEt_2)_2$ (1.0 g, 3.4 mmol) in THF (30 mL), and the reaction mixture was stirred for 30 min. $[Pd(CH_3CN)_4](BF_4)_2$ (1.51 g, 3.4 mmol) in acetonitrile (20 mL) was added to the THF solution. The reaction mixture was stirred for an additional 30 min, and then the solvent was removed on a vacuum line. The resulting solid was washed with hexanes and redissolved in acetonitrile (30 mL). Aqueous HBF_4 (0.1 mL, 9.6 M) was added to this solution, and then the solution was warmed to 60 °C for 2 h. The solvent was removed on a vacuum line, and the resulting solid was washed with diethyl ether. Precipitation of the product from a mixture of acetonitrile and diethyl ether produced a light yellow powder (1.54 g, 60%) which was isolated by filtration. Characterization data are given in Tables 2 and 3.

Results

Synthesis and Characterization of Ligands and Palladium Complexes. The ligands **3a−3c** were prepared as shown in eq 1. In the first step, vinylmagnesium bromide reacts with dichloromesitylphosphine to form divinylmesitylphosphine (**2**). In the next step, the triphosphine ligands are formed by P−H addition[19] of the corresponding secondary phosphine to the carbon double bond of divinylmesitylphosphine. These ligands

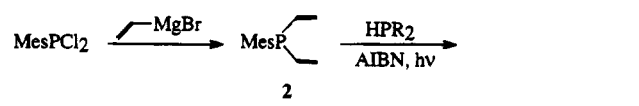

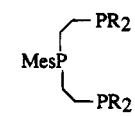

(1)

3a, MesetpE R = Et
3b, Mesetp R = Ph
3c, MesetpC R = Cy

were characterized by ^1H and ^{31}P NMR spectroscopy (Table 2). The ^1H NMR data, while consistent with the ligand formulations, are not as diagnostic as the ^{31}P NMR spectra. Each triphosphine ligand exhibits a doublet and a triplet resonance in their ^{31}P NMR spectra assigned to the terminal and central phosphorus atoms, respectively. The coupling constants of 25−35 Hz are in the range expected for three-bond P−P coupling for free ligands, and the chemical shifts calculated using standard equations and empirical constants for various substituents[20] agree well with the observed values (see Table 2).

Ligand **6** was prepared according to eq 2. In the first step, diethylphosphine adds across the carbon double bond of divinyl(diethylamino)phosphine to form a tri-

(19) King, R. B. *Catalytic Aspects of Metal Phosphine Complexes*, Alyea, E. C., Meek, D. W., Eds.; Advances in Chemistry Series 196; American Chemical Society: Washington, DC, 1982; p 313.

(20) Fluck, E.; Heckmann, G. *Phosphorus-31 NMR Spectroscopy in Stereochemical Analysis*; Verkade, J. G., Quin, L. D., Eds.; Methods in Stereochemical Analysis Series No. 8; VCH: Deerfield Beech, FL, 1987; pp 88−93.

phosphine ligand with a diethylamino substituent on the central phosphorus atom, **4**. Subsequent reaction with methanol produces the methoxy derivative **5**, which reacts with lithiated trimethoxybenzene to form **6**. The ^{31}P NMR spectrum of **6** consists of the expected doublet and triplet (Table 2).

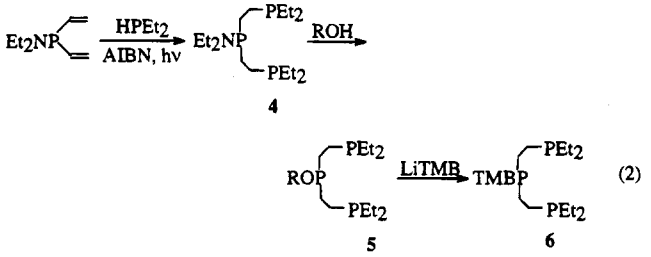

(2)

Reaction of ligands **3a–c** with $[Pd(CH_3CN)_4](BF_4)_2$ results in the formation of the corresponding [Pd(MesetpR)(CH_3CN)[$(BF_4)_2$ complexes **7a–c** as shown in eq 3.

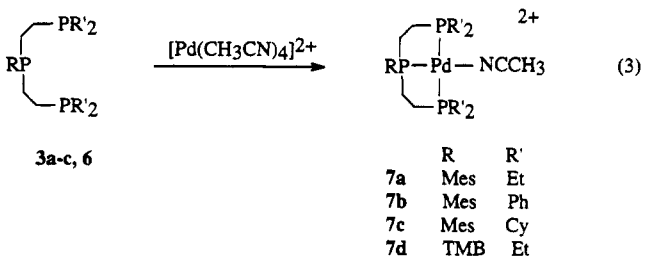

(3)

	R	R'
7a	Mes	Et
7b	Mes	Ph
7c	Mes	Cy
7d	TMB	Et

To obtain the analogous [Pd(TMBetpE)(CH_3CN)]$(BF_4)_2$ complex **7d**, the product obtained from the reaction between $[Pd(CH_3CN)_4](BF_4)_2$ and the crude ligand **6** must be treated with HBF_4. The acid presumably cleaves a base that is a contaminant in the preparation of **6**. The overall synthesis of **7d** is reasonably efficient.

^1H NMR spectra of complexes **7a,c** exhibit three distinct methyl resonance for the mesityl substituent in a 1:1:1 ratio at room temperature. Raising the temperature causes two of the methyl resonances to collapse to a single resonance. For complexes **7b,d**, the NMR samples must be cooled to 0 and −80 °C, respectively, to stop rotation of the mesityl and trimethoxybenzene rings. Resonances assigned to the methyl group of coordinated acetonitrile are observed in noncoordinating solvents such as nitromethane-d_3 (Table 2). These resonances shift toward the position of free acetonitrile when excess acetonitrile is added. This indicates the acetonitrile ligands exchange rapidly at room temperature with free acetonitrile. In dimethylformamide, the acetonitrile resonances occur at the position of uncoordinated acetonitrile indicating displacement of acetonitrile by this solvent. The presence of coordinated acetonitrile in these complexes is also indicated by the observation of two bands at approximately 2290 cm^{-1} and 2320 cm^{-1} in the infrared spectra of these complexes in the solid state or in dichloromethane solutions (Table 3). These two bands are assigned to CN stretching and combination modes, respectively.[21]

The ^{31}P NMR spectra of complexes **7a–d** all exhibit doublet and triplet resonances assigned to the central and terminal phosphorus atoms of the triphosphine ligands (Table 2). Particularly noteworthy are the chemical shifts for the central phosphorus atom. The similarity of the value observed for **7d** (92.09 ppm) to those of **7a–c** (96–99 ppm) suggests that the oxygen atoms of the *o*-methoxy groups do not coordinate to palladium. The formation of a third five-membered ring in this complex should result in a significant (~20 ppm) downfield shift of this resonance if a strong Pd–O bond is formed.[22] The spectral data of these complexes support their formulation as square-planar palladium complexes.

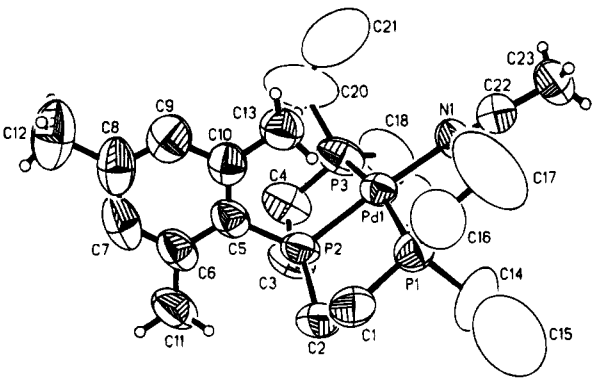

Figure 1. Drawing of the $[Pd(MesetpE)(CH_3CN)]^{2+}$ cation of **7a**, showing the atom-numbering scheme. Anisotropic thermal ellipsoids are shown at the 50% probability level. Hydrogen atoms, except those that were refined as rigid groups, are omitted for clarity.

Table 4. Selected Bond Distances (Å) and Bond Angles (deg) for [Pd(MesetpE)(CH_3CN)]$(BF_4)_2$ (7a)

Bond Distances			
Pd(1)–P(1)	2.324(2)	Pd(1)–P(2)	2.231(2)
Pd(1)–P(3)	2.338(2)	Pd(1)–N(1)	2.057(6)
P(1)–C(1)	1.813(8)	P(1)–C(14)	1.984(14)
P(1)–C(16)	1.807(9)	P(2)–C(2)	1.827(7)
P(2)–C(3)	1.825(8)	P(2)–C(5)	1.827(6)
P(3)–C(4)	1.809(8)	P(3)–C(18)	1.779(10)
P(3)–C(20)	1.897(11)	N(1)–C(22)	1.119(9)
C(1)–C(2)	1.525(10)	C(22)–C(23)	1.471(10)
Bond Angles			
P(1)–Pd(1)–P(2)	84.9(1)	P(1)–Pd(1)–P(3)	164.9(1)
P(2)–Pd(1)–P(3)	84.2(1)	P(1)–Pd(1)–N(1)	95.0(2)
P(2)–Pd(1)–N(1)	176.6(1)	P(3)–Pd(1)–N(1)	95.1(2)
Pd(1)–P(1)–C(1)	106.8(2)	Pd(1)–P(1)–C(14)	102.0(4)
C(1)–P(1)–C(14)	105.1(5)	Pd(1)–P(1)–C(16)	121.1(3)
Pd(1)–P(2)–C(2)	108.6(2)	Pd(1)–P(2)–C(3)	103.3(2)
Pd(1)–P(2)–C(5)	116.3(2)	Pd(1)–N(1)–C(22)	176.3(5)
N(1)–C(22)–C(23)	177.0(7)	C(5)–C(10)–C(13)	125.6(5)
C(5)–C(6)–C(11)	126.6(6)		

Structural Characterization of [Pd(MesetpE)(CH_3CN)]$(BF_4)_2$ (7a). An X-ray diffraction study of this complex was carried out to investigate the interaction between palladium and the *o*-methyl groups of the mesityl substituent. Crystals of **7a** suitable for structure determination were obtained by layering ether on top of an acetonitrile solution of the complex. The crystals consist of $[Pd(MesetpE)(CH_3CN)]^{2+}$ cations and BF_4^- anions. A drawing of the cation is shown in Figure 1, and Table 4 lists selected bond distances and bond angles of the cation. The drawing illustrates the square-planar structure of the cation with one methyl group of the mesityl substituent blocking a potential coordination site above the plane of the complex. The interaction between the methyl group and the palladium atom appears to be repulsive, with the plane of the mesityl

(21) Storkhoff, B. N.; Lewis, H. C., Jr. *Coord. Chem. Rev.* **1977**, *23*, 1.

(22) Garrou, P. E. *Chem. Rev.* **1981**, *81*, 229.

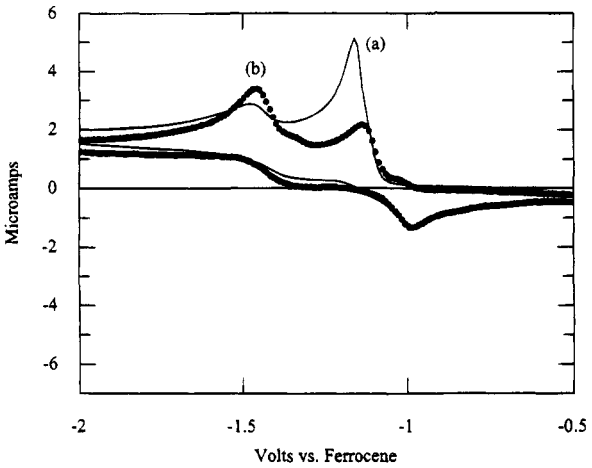

Figure 2. Cyclic voltammograms of a 2.0×10^{-3} M solution of $[Pd(Mesetp)(CH_3CN)](BF_4)_2$ (**7b**) in DMF at 100 mV/s: (a) under N_2 (solid line); (b) after saturating with CO_2 (solid circles).

group twisted slightly with respect to the plane that bisects the complex. The bond distance of the central phosphorus atom to palladium, Pd–P(2), is approximately 0.1 Å shorter than the Pd–P bond lengths to the two terminal phosphorus atoms. Other structurally characterized complexes containing chelating triphosphine ligands show a similar shortening of the bond between the central phosphorus atom and the metal.[23] The P(2)–Pd–P(1) and P(2)–Pd–P(3) angles of 84.9 and 84.2° are typical of diphosphine ligands containing a bridging ethylene linkage.[24] The steric constraints imposed by the two five-membered chelate rings result in a small P(1)–Pd–P(3) angle of 164.9° and P(1)–Pd–N(1) and P(3)–Pd–N(1) angles greater than 90°. The Pd–N(1) bond distance is in the range expected for a second row transition metal complex of acetonitrile.[21]

Electrochemical Studies. The cyclic voltammogram of $[Pd(Mesetp)(CH_3CN)](BF_4)_2$ (**7b**) shown by trace a in Figure 2, is typical of these complexes. Two cathodic waves are observed at −1.16 and −1.47 V vs the ferrocene/ferrocenium couple. The small anodic wave observed at −0.99 V under a nitrogen atmosphere is coupled to the wave at −1.16 V. This wave persists when the direction of the scan is reversed immediately after traversing the wave at −1.16 V, and it is larger relative to the cathodic wave at −1.16 V at higher scan rates. Similarly, the relative magnitude of the wave at −1.47 V first increases and then decreases when the scan rate is increased. These results indicate the unknown species responsible for the two waves at −1.47 and −0.99 V are unstable. The cathodic wave at −1.16 V is diffusion-controlled as shown by a linear plot of the current vs the square root of the scan rate between 0.05 and 4 V/s. This wave is assigned to two closely spaced one-electron reductions. This assignment is based on the magnitude of the current observed for this wave by cyclic voltammetry and the charge passed during chronoamperometric experiments. The complex $[Pd(etp)(PEt_3)](BF_4)_2$ (where etp is bis((diphenylphosphino)ethyl)phenylphosphine) has been shown to undergo a reversible two-electron reduction[7] and should have a diffusion coefficient nearly identical with that of **7b**. The ratio of the peak current of the cathodic wave at −1.16 V of **7b** to the peak current of the two-electron reduction wave of $[Pd(etp)(PEt_3)](BF_4)_2$ is 0.95 for solutions of the same concentration. Linear chronocoulometric plots of charge versus $t^{1/2}$ for **7b** and $[Pd(etp)(PEt_3)](BF_4)_2$ also have nearly identical slopes ([slope of **7b**]/[slope of $[Pd(etp)(PEt_3)](BF_4)_2$] = 0.93). These results indicate that the number of electrons transferred during the reduction of these two compounds is the same, and consequently the reduction wave at −1.16 V for **7b** involves two electrons. In the presence of CO_2, the peak at −1.16 V shifts in a positive direction and decreases in height as shown in Figure 2, trace b. The ratio of the peak current for the first cathodic wave of **7b** under CO_2 to the peak current observed under nitrogen is 0.54. The decrease in height and shift in potential of this wave is attributed to a rapid reaction of the one-electron reduction product of **7b**, $[Pd(Mesetp)(DMF)]^+$, with CO_2. A second electron transfer does not occur until −1.46 V. The identity of the species responsible for the wave at −1.46 V under CO_2 is again not known. Although the potential is nearly the same as the −1.47 V wave observed for **7b** under nitrogen, the relative magnitude of this wave is much larger, and the species formed under CO_2 appears to be more stable. The wave at −1.46 V may correspond to a Pd^I–CO_2 adduct, or it may be the same species observed at −1.47 V under nitrogen whose formation is promoted by CO_2. Because of the transient nature of these intermediates and our inability to isolate and fully characterize them, further speculation on the identity of the complexes giving rise to these waves is unwarranted. In any case, the important feature is that the reduction of **7b** under nitrogen corresponds to a two-electron process while only one electron per palladium is consumed in the presence of CO_2. This observation indicates that a Pd(I) and not a Pd(0) species is the active intermediate in reactions with CO_2. The other complexes shown in Table 5 exhibit electrochemical properties similar to those observed for **7b**.

Controlled-potential electrolyses of **7a–d** at potentials 100 mV negative of their half-wave potentials resulted in the passage of 0.6–1.5 faradays of charge per mole of complex as shown in Table 5 with formation of a mixture of products. These reductions do not result in clean formation of Pd(I) dimers, as observed previously for $[Pd(triphosphine)(CH_3CN)](BF_4)_2$ complexes with less bulky central substituents.[7]

Catalytic Studies. Cyclic voltammograms of $[Pd(MesetpE)(DMF)](BF_4)_2$ in the presence of both HBF_4 and CO_2 (trace a) and in the presence of HBF_4 only (trace b) are shown in Figure 3. A catalytic wave is observed for DMF solutions containing complex, acid, and CO_2. Controlled-potential electrolysis at −1.42 V on solutions containing $[Pd(MesetpE)(DMF)](BF_4)_2$ (1.0×10^{-3} M), HBF_4 (0.1 M), and CO_2 (0.18 M) produces CO and H_2. The amounts of CO and H_2 produced were measured by gas chromatography. Current efficiencies for CO (85%) and H_2 (19%) production were calculated assuming 2 electrons/mol of CO and H_2. Factors influencing selectivity will be discussed in more detail below.

For a reversible electron-transfer reaction followed by a fast catalytic reaction at high substrate concentrations, the ratio between the limiting catalytic current,

(23) Saum, S. E.; Laneman, S. A.; Stanley, G. G. *Inorg. Chem.* **1990**, *29*, 5065.

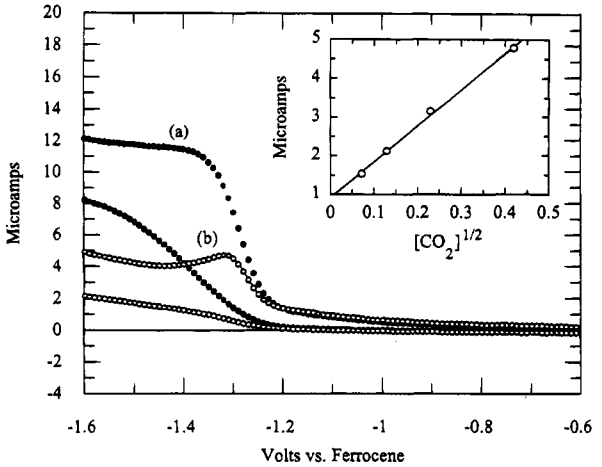

Figure 3. Cyclic voltammogram of a 1.0×10^{-3} M solution of [Pd(MesetpE)(CH_3CN)](BF_4)$_2$ (**7a**) in DMF containing 0.1 M HBF_4: (a) saturated with CO_2 (solid circles); (b) after purging with N_2 (open circles). Inset graph shows a plot of catalytic current as a function of the square root of the CO_2 concentration for a DMF solution containing 0.6×10^{-3} M [Pd(MesetpE)(CH_3CN)](BF_4)$_2$ and 0.1 M HBF_4. Scan rates were all 50 mV/s.

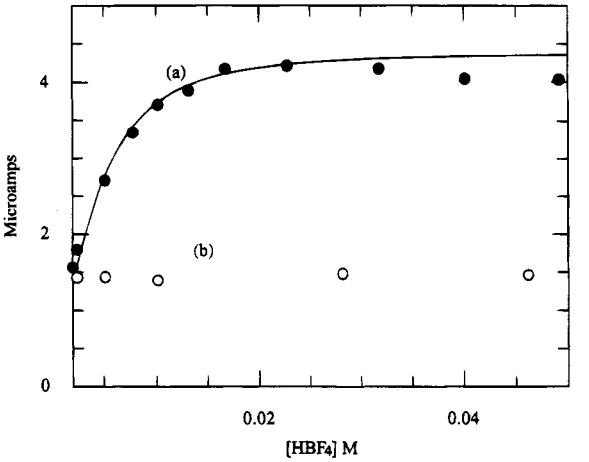

Figure 4. Plot showing the dependence of the peak or plateau current on acid concentration for a 0.6×10^{-3} M solution of [Pd(MesetpE)(CH_3CN)](BF_4)$_2$ (**7a**) in DMF: (a) under CO_2 (solid circles); (b) solution purged with N_2 (open circles). The solid line represents i_c calculated using eq 5 with $k_1 = 39$ and $k_2 = 1.8 \times 10^5$. Scan rates were all 50 mV/s.

i_c, and the peak current due to reversible reduction of the catalyst, i_d, is given by eq 4.[24] In eq 4, n is the

$$\frac{i_c}{i_d} = \frac{\sigma}{0.447}\sqrt{\frac{RT}{nF}}\sqrt{\frac{kC'_z{}^m}{v}} \qquad (4)$$

number of electrons involved in catalyst reduction, k is the rate constant, v is the scan rate, C_z is the concentration of substrate(s), m is an exponential corresponding to the reaction order of the substrate, and σ is a factor which depends on the mechanism. From this equation, it can be seen that a plot of the catalytic current versus the square root of the CO_2 concentration should be linear if the reaction is first order in CO_2. Such a plot is shown in the inset graph of Figure 3. The catalytic current also shows a linear dependence on the catalyst concentration consistent with a reaction that is first order in catalyst. These results are consistent with a rate determining reaction of CO_2 with the Pd(I) species, $[Pd(MesetpE)(DMF)]^+$, formed on reduction of $[Pd(MesetpE)(DMF)]^{2+}$.

The dependence of the catalytic current on acid concentration is shown in Figure 4, trace a. At low acid concentrations, the current exhibits a linear dependence on acid concentration, whereas at high acid concentrations, the current reaches a limiting value that is independent of acid concentration. This behavior indicates saturation kinetics expected for a catalytic cycle, and eq 4 must be modified to account for this behavior. For two rate-determining steps, one first order in CO_2 and the other second order in acid, the pseudo-first-order rate constant, kC_z, can be replaced by the expression shown in the second square-root bracket of eq 5.[7,25] In this equation, k_1 is the second-order rate constant for the reaction of CO_2 with the Pd(I) intermediate, and k_2 is a third-order rate constant which is undoubtedly not a simple rate constant. The dependence of the

$$\frac{i_c}{i_d} = \frac{\sigma}{0.447}\sqrt{\frac{RT}{nFv}}\sqrt{\frac{k_1k_2[CO_2][H^+]^2}{k_1[CO_2] + k_2[H^+]^2}} \qquad (5)$$

catalytic current on acid, CO_2, and catalyst concentrations is the same as that observed previously for other [Pd(triphosphine)(DMF)](BF_4)$_2$ complexes.[7] Therefore, introduction of the bulky mesityl group does not appear to significantly affect the mechanism of the catalytic reaction.

Second-order rate constants for catalytic reactions can be calculated using either eq 4 or 5. However, there is an ambiguity in the values of the rate constants, depending on the value used for σ. If the second electron transfer occurs in solution—a SET mechanism—the value of σ is $\sqrt{2}$. If the second electron transfer occurs at the electrode surface—an ECE mechanism—the value of σ is 2. Assuming an incorrect mechanism could lead to the calculated rate constant being in error by a factor of 2.[24,26] In previous work, we have used eq 4 with a σ value of 2 to calculate rate constants for the reaction of $[Pd(triphosphine)(DMF)]^+$ complexes with CO_2.[7] Reasonable agreement between rate constants obtained by this method and an independent method was observed. The latter method relied on shifts of the cathodic peak potential in the presence of CO_2.[27] The rate constants shown in Table 5 were also calculated using eq 4 with a σ value of 2. This allows a direct comparison of our new rates with those reported previously. These rate constants are a factor of 2 smaller than those which would be obtained assuming a SET mechanism.

Catalyst Selectivity. As discussed above, the current efficiencies for the catalysts shown in Table 5 were determined by performing controlled potential electrolysis experiments coupled with a quantitative analysis of

(24) Savéant, J.-M.; Vianello, E. *Electrochim. Acta* **1965**, *10*, 905. Hammouche, M.; Lexa, D.; Momenteau, M.; Savéant, J.-M. *J. Am. Chem. Soc.* **1991**, *113*, 8455.

(25) Huang, C. Y. In *Contemporary Enzyme Kinetics and Mechanism*; Purich, D. L., Ed.; Academic Press: New York, 1983; pp 1–31. King, E. L.; Altman, C. *J. Phys. Chem.* **1956**, *60*, 1375.

(26) Savéant, J.-M.; Su, K. B. *J. Electroanal. Chem.* **1985**, *196*, 1.

(27) Nicholson, R. S.; Shain, I. *Anal. Chem.* **1964**, *36*, 706.

Table 5. Electrochemical Data for $[RP(CH_2CH_2PR'_2)_2Pd(CH_3CN)](BF_4)_2$ Complexes in Dimethylformamide

R, R'	$E_{1/2}$ (V)[a]	k (M^{-1} s^{-1})	current efficiency CO	current efficiency H_2	turnover no.[b]	n[c]
Mes, Et (**7a**)	−1.32	39	85	19	>40	1.5
Mes, Ph (**7b**)	−1.08	4	88	14	>26	1.9
Mes, Cy (**7c**)	−1.24	14	76	26	>36	1.1
TMB, Et (**7d**)	−1.47	188	61	45	>25	0.6

[a] Reduction potentials are reported relative to the internal standard ferrocene. [b] The turnover number is defined as the moles of CO produced/mol of catalyst. [c] faradays/mol of $[Pd(triphosphine)(CH_3CN)](BF_4)_2$ under N_2 in the absence of HFB_4.

the products by gas chromatography. Within experimental error (approximately 5%), all of the charge passed can be accounted for by the H_2 and CO formed. In DMF solutions containing 0.1 M HBF_4, the selectivity for $[Pd(etpC)(CH_3CN)](BF_4)_2$ was 97% for CO, and if the weaker acid, H_3PO_4, is used instead of HBF_4 a slightly higher value of 99% was obtained. By using the combination of $[Pd(etpC)(CH_3CN)](BF_4)_2$, H_3PO_4, and dimethylformamide, nearly quantitative selectivity for CO production can be obtained. It was found during the course of these studies that the history of the solvent had a significant effect on the observed current efficiencies. For example, when controlled-potential electrolyses of $[Pd(MetpE)(CH_3CN)](BF_4)_2$ and $[Pd(MetpC)(CH_3CN)](BF_4)_2$ (where MetpE is bis((diethylphosphino)ethyl)methylphosphine and MetpC is bis((dicyclohexylphosphino)ethyl)methylphosphine) were carried out using dimethylformamide exposed to the atmosphere for several weeks, the current efficiencies for CO production were observed to be 10% and 13%, respectively.[7] Using dimethylformamide that had been stored under a nitrogen atmosphere resulted in much higher current efficiencies of 70% and 92%, respectively. Addition of formic acid and dimethylamine to solutions of $[Pd(MetpC)(CH_3CN)](BF_4)_2$ in DMF resulted in current efficiencies of 74% and 94%, respectively, for CO production. Although formic acid has a detrimental effect on catalyst selectivity, it is unlikely that it is solely responsible for the low selectivity observed for DMF solutions exposed to air, because ^{13}C and ^1H NMR spectra of these aged solutions do not indicate concentrations of formic acid as high as for DMF stored under nitrogen and spiked with formic acid. Studies using propylene carbonate as the solvent resulted in reduced selectivity for CO (approximately 15%) and the formation of small amounts of methane.[28]

Discussion

To study the possibility of a sixth ligand coordinating in a transition state such as **1**, three complexes, **7a−c**, were prepared which would block coordination of a sixth ligand trans to coordinated CO_2. Another complex, **7d**, which should promote six-coordination, was also prepared. The syntheses of ligands **3a−c** are straightforward and utilize the free-radical addition of PH bonds to activated carbon double bonds to form the triphosphine structure. In the synthesis of **6**, the most successful route involved assembling a triphosphine framework followed by substitution of the methoxide group bound to the central phosphorus atom with the trimethoxyphenyl anion (eq 2). The corresponding $[Pd(triphosphine)(CH_3CN)](BF_4)_2$ complexes are readily obtained by reacting the ligands with $[Pd(CH_3CN)_4](BF_4)_2$.

Previous structural and spectroscopic studies of five- and six-coordinate rhodium complexes suggested that a bulky substituent on the central phosphorus atom would preclude six-coordination.[30] Figure 1 shows that one of the *o*-methyl groups of $[Pd(MesetpE)(CH_3CN)](BF_4)_2$ clearly blocks one possible coordination site in the solid state. The observation of three methyl resonances in the ^1H NMR spectrum indicates that this structure is also preserved in solution. These data show that coordination of a sixth ligand for complexes **7a−c** should be very unlikely. In contrast, the close proximity of the methoxy group in **7d** to palladium should favor six-coordination in intermediates such as **1**.

Kinetic studies were carried out on $[Pd(MesetpE)(CH_3CN)](BF_4)_2$ to determine if the bulky mesityl substituent of complexes **7a−c** resulted in a change in the mechanism for CO_2 reduction from that observed previously for $[Pd(triphosphine)(CH_3CN)](BF_4)_2$ complexes.[7] The same dependence of the catalytic current on catalyst, CO_2, and acid concentrations indicates the same mechanism. The rate-determining step at HBF_4 concentration greater than 0.02 M is first order in catalyst and first order in CO_2. In the presence of CO_2 but no acid, the peak current for this complex corresponds to a one-electron reduction and the peak potential shifts in a positive direction. This is further evidence that the rate-determining step is the reaction of CO_2 with the palladium(I) species, $[Pd(MesetpE)(DMF)]^+$. The intermediate formed by this reaction should have a structure similar to that shown for **1**. Coordination of a sixth ligand to such an intermediate is prevented by the steric bulk of the mesityl group.

Figure 5 shows a plot of the log of catalytic rates vs the redox potential for $[Pd(triphosphine)(CH_3CN)](BF_4)_2$ complexes described in this and a previous study.[7] The best-fit line for complexes with either methyl or phenyl substituents on the central phosphorus atom is shown

(28) Using CO_2 spiked with $^{13}CO_2$, GC/MS studies confirmed that the methane produced arises from CO_2. In addition to methane, CO and hydrogen are also formed. When CO was used as the gas instead of CO_2, no methane was produced, indicating that free CO is not an intermediate. Electrolyses carried out with pure carbon or pure silver electrodes in the presence of $[Pd(etpC)(CH_3CN)](BF_4)_2$ produced no methane. Electrolyses performed using carbon/silver electrodes in the absence of $[Pd(etpC)(CH_3CN)](BF_4)_2$ also failed to produce methane. Only when reticulated vitreous carbon electrodes containing silver wire or silver epoxy and $[Pd(etpC)(CH_3CN)](BF_4)_2$ were present was methane formed. Because copper electrodes are known to reduce CO_2 to methane under much different conditions, care was taken to eliminate all sources of copper in this system. Other attempts to optimize this system for methane production indicated that the highest current efficiencies were observed when the solutions were not stirred, and that decreasing the acid concentration from 0.1 M HBF_4 to 0.05 M resulted in a decrease in the current efficiency from 11 to 7%. The highest current efficiency observed was 11% assuming 8 electrons/mol of methane produced. Although the potential of this system is significantly positive of that observed for copper electrodes (−1.3 V vs −2.0 V;[29] all potentials are with respect to the ferrocene/ferrocenium couple), the current efficiency is less (11% under the best conditions for our system vs 65−70% for copper electrodes), and the chemistry appears to be even more complex.

(29) Hori, Y.; Kikuchi, K.; Suzuki, S. *Chem. Lett.* **1985**, 1695. Hori, Y.; Murata, A.; Takahashi, R.; Suzuki, S. *J. Am. Chem. Soc.* **1987**, *109*, 5022. Sammells, A. F.; Cook, R. L. *Electrochemical and Electroanalytic Reactions of Carbon Dioxide*; Sullivan, B. P., Krist, K., Guard, H. E., Eds.; Elsevier: New York, 1993; p 217. Frese, K. W., Jr. *Ibid.*, p 145.

(30) Napier, T. E.; Meek, D. W.; Kirchner, R. M.; Ibers, J. A. *J. Am. Chem. Soc.* **1973**, *95*, 4194. Meek, D. W.; DuBois, D. L.; Tiethof, J. *Inorganic Compounds with Unusual Properties*; King, R. B., Ed.; ACS Symposium Series 150; American Chemical Society: Washington, DC, 1976; p 335.

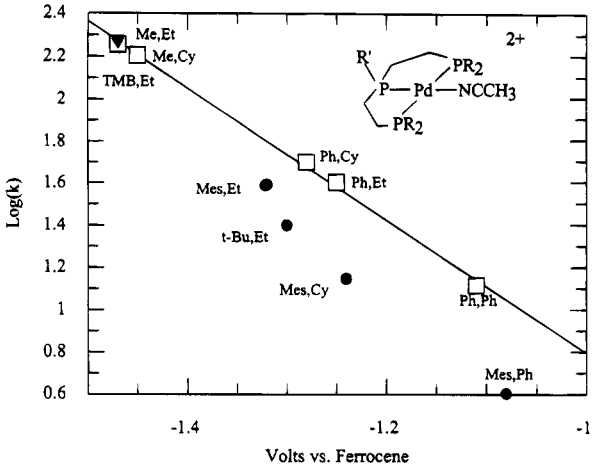

Figure 5. Plots of the log of the second-order rate constants measured for $[R'P(CH_2CH_2PR_2)_2Pd(CH_3CN)](BF_4)_2$ complexes versus the half-wave potential of the catalysts. Open boxes are for complexes with phenyl or methyl substituents on the central phosphorus atom of the triphosphine ligand. Solid circles are for complexes with *tert*-butyl or mesityl substituents on the central phosphorus atom. The solid triangle is for complex **7d** with a trimethoxyphenyl substituent on the central phosphorus atom.

in Figure 5. For these complexes, relatively little steric interaction with CO_2 is expected based on space-filling models. The rate constants of complexes **7a**–**c** and of $[Pd(BetpE)(CH_3CN)](BF_4)_2$ (where BetpE is bis((diethylphosphino)ethyl)-*tert*-butylphosphine) lie below this line. The rates of these complexes are about half those expected from their potentials. In these complexes, a methyl group of either the mesityl or *tert*-butyl group should block one coordination site. If coordination of a sixth ligand were playing an important role in stabilizing intermediates such as **1**, the rate constants for **7a**–**c** and $[Pd(BetpE)(CH_3CN)](BF_4)_2$ should be dramatically reduced. The small decrease in rate constants by a factor of 2 is more consistent with one of the two faces of the catalytic molecule being inaccessible to CO_2 attack. From these results, we also conclude that CO_2 approaches the catalyst along the axis perpendicular to the plane of the catalyst. If this is the direction of approach, then a bulky group on the central phosphorus atom of the triphosphine ligand would be expected to retard the rate of the reaction, as is observed. If CO_2 approached along the axis containing the solvent molecule, then bulkier substituents on the terminal phosphorus atoms would be expected to result in a decrease in the rate. However, as can be seen from Figure 5, replacement of terminal ethyl substituents with more bulky cyclohexyl substituents has no detectable effect on the rate of the reaction. As discussed above, the observation that the solvent appears to remain coordinated prior to reaction with CO_2 also makes the approach of CO_2 along this axis seem less likely.

The rate constant for $[Pd(TMBetpE)(CH_3CN)](BF_4)_2$ (**7d**) is close to the value expected on the basis of its reduction potential (see Table 5 and Figure 5). This complex was designed to promote coordination of the oxygen atom of a methoxy group in an intermediate such as **1**. The failure to observe a significant increase in the catalytic rate for this complex suggests that coordination of a sixth ligand does not occur for the intermediate formed from **7d** or that such an intermediate does not lead to significantly enhanced catalytic rates.

In summary, $[Pd(MesetpR)(CH_3CN)](BF_4)_2$ complexes have been prepared that preclude the formation of six-coordinate transition states or intermediates. Mechanistic studies and a comparison of the rate constants of these complexes support a five-coordinate transition state for the rate-determining step in which CO_2 approaches along the axis perpendicular to the plane of the catalyst. Studies of factors affecting the selectivity of these catalysts resulted in a system that forms CO in nearly quantitative yields.

Acknowledgment. This work was supported by the United States Department of Energy, Office of Basic Energy Sciences, Chemical Sciences Division.

Supplementary Material Available: Table 1s, containing crystal data, data collection conditions, and solution and refinement details of $[Pd(MesetpE)(CH_3CN)](BF_4)_2$, and Tables 2s–6s, giving atomic coordinates and equivalent isotropic displacement parameters, bond lengths, bond angles, anisotropic displacement parameters, and hydrogen atom coordinates and isotropic parameters (13 pages). Ordering information is given on any current masthead page.

OM940382F